NMRlipids IV: Headgroup & glycerol backbone structures, and cation binding in bilayers with PS lipids

Pavel Buslaev,[1] Fernando Favela,[2] Tiago M. Ferreira,[3] Ivan Gushchin,[1] Matti Javanainen,[4] Batuhan Kav,[5] Jesper J. Madsen,[6] Markus Miettinen,[5] Josef Melcr,[4] Ricky Nencini,[4] O. H. Samuli Ollila,[4,7,*] and Thomas Piggot 1.Authorlist is not yet complete[8]

[1]*Moscow Institute of Physics and Technology*
[2]*Mexico*
[3]*Halle, Germany*
[4]*Institute of Organic Chemistry and Biochemistry, Academy of Sciences of the Czech Republic, Prague 6, Czech Republic*
[5]*Department of Theory and Bio-Systems, Max Planck Institute of Colloids and Interfaces, 14424 Potsdam, Germany*
[6]*Department of Chemistry, The University of Chicago, Chicago, Illinois 60637, United States of America*
[7]*Institute of Biotechnology, University of Helsinki*
[8]*Southampton, United Kingdom*

(Dated: February 6, 2019)

Phosphatidylserine (PS) is the most common negatively charged lipid in eykaryotic membranes. PS lipids interact with signaling and other proteins via electrostatic interactions and direct binding, and induce membrane fusion and phase separation together with calcium ions. Molecular details of these phenomena are not well understood because accurate models to interpret the experimental data has not been available. Here, we collect a set of experimental NMR data which can be used together with molecular dynamics (MD) simulations to interpret the lipid headgroup structures and details of ion binding in pure PS and mixed PS:PC lipid bilayers. We use the open collaboration method to collect data from available MD simulation models of PS lipids. None of the models reproduce the NMR data with experimental accuracy, but the best models suggest that the carboxyl group in the serine headgroup does not rotate freely. In line with the previous results for PC lipids, none of the tested force fields correctly captures the cation binding affinity to lipid bilayers containing PS lipids. In contrast to PC lipids, the response of PS headgroups to the bound ions qualitatively differs from experiments in the tested MD simulation models. The collected experimental dataset and simulation results pave the way for improvement of lipid force fields to correctly describe negatively charged membranes and their interactions with ions. The work is performed in the NMRlipids open collaboration project (`nmrlipids.blogspot.fi`).

INTRODUCTION

Phosphatidylserine (PS) is the most common negatively charged lipid in eykaryotic membranes. PS lipids compose 8.5% of total lipid weight of erythrocytes, but the abundance varies between different organelles up to 25-35% in the cytosolic leaflet of plasma membranes [1–3]. Despite of the relatively low abundance, PS lipids are important signaling molecules. They interact with signaling proteins [2], regulate surface charge and protein localization [4], and induce protein aggregation [5, 6]. Some protein domains spesifically interact PS lipids, while others are attracted by general electrostatics and the binding can be regulated by calcium [2]. Therefore, the structural details of lipid headgroups and the details of cation binding are crucial for the PS mediated signaling processes.

Previous experimental studies have concluded that PS headgroups are more rigid than phophocholines (PC) due to the hydrogen bonding network or electrostatic interactions [7, 8]. Multivalent cations and Li^+ are able to form strong dehydrated molecular complexes with PS lipids, while monovalent ions interact more weakly with PS containing bilayers [9–19]. The dehydrated complexes of PS headgroup and calcium ions can also lead to the phase separation [9, 10, 14–18]. On the other hand, some studies propose that the specific binding affinity is similar to the negatively charged and zwitterionic lipids and that the increased cation binding to negatively charged lipid bilayer arise only due to the increase of local cation concentration in the vicinity of membranes [20, 21]. Dilution of bilayers with PC lipids makes PS headgroups less rigid and reduces propensity for the formation of strong complexes with multivalent ions [7, 8, 17, 18]. The molecular level interpretation of these observations is, however, not available.

Several classical molecular dynamics (MD) simulation studies are done to understand PS headgroups, their influence on lipid bilayer properties and interactions with ions [19, 22, 34, 49–59]. However, the results strongly depend on the used force field parameters. For example, the recent simulations using NBfix parameters for calcium [60] in CHARMM36 force field [22, 61] combined with 2D infrared spectroscopy suggests that calcium ions interacts only with the carboxylate group of PS lipids [58], while the same force field without the NBfix parameters together with the NMR chemical shifts and REDOR experiments suggests a significant binding affinity also to the phosphate region [59]. On the other hand, simulations with the Berger force field [34, 62] combined with fluorescent and vibrational sum frequency spectroscopy suggested a significant calcium binding also to the carbonyls in the acyl chains [57]. We have recently demonstrated that such controversies can be resolved by comparing C-H bond order parameters of lipid headgroups between simulations and experiments [63, 64], which can be directly measured from NMR experiments with high accuracy and compared to simulations in order to evaluate the simulation model quality or to interpret the experiments [65]. Previous studies showed that the structure of PC lipid headgroup

TABLE I: The list of MD simulations of pure PS bilayers without additional salt. Simulation details are given in the supplementary information

lipid/counter-ions	force field for lipids / ions	[a]N_l	[b]N_w	[c]N_c	[d]T (K)	[e]t_{sim}(ns)	[f]t_{anal} (ns)	[g]files
POPS/Na^+	CHARMM36 [22]	128	4480	0	298	500	100	[23]
POPS/K^+	CHARMM36 [22]	128	4480	0	298	500	100	[24]
POPS/Na^+	CHARMM36ua [**?**] 2.	128	4480	0	298	500	100	[25]
POPS/Na^+	MacRog [26]	128	4480	0	298	500	100	[27]
POPS/K^+	MacRog [26]	128	4480	0	298	200	150	[28]
POPS/Na^+	lipid17 [29] / JC [30]	128	4480	0	298	600	100	[31]
POPS/Na^+	lipid17 [29] / ff99 [32]	128	4480	0	298	600	100	[33]
POPS/Na^+	Berger [34**?**]	128	4480	0	298	500	100	[35]
POPS/Na^+	GROMOS-CKPM [**?**] 3.	128	4480	0	298	500	100	[36]
POPS/Na^+	GROMOS-CKP [**?**] 4.	128	4480	0	298	500	100	[37]
POPS/Na^+	Slipids [38]	128	4480	0	298	500	100	[39]
DOPS/Na^+	CHARMM36 [22]	128	4480	0	303	500	100	[40]
DOPS/Na^+	CHARMM36ua [**?**] 5.	128	4480	0	303	500	100	[41]
DOPS/Na^+	lipid17 [29] / JC [30]	128	4480	0	303	600	100	[42]
DOPS/Na^+	lipid17 [29] / ff99 [32]	128	4480	0	303	600	100	[43]
DOPS/Na^+	Berger [34**?**]	128	4480	0	303	500	100	[44]
DOPS/Na^+	GROMOS-CKPM [**?**] 6.	128	4480	0	303	500	100	[45]
DOPS/Na^+	GROMOS-CKP [**?**] 7.	128	4480	0	303	500	100	[46]
DOPS/Na^+	Slipids [38]	128	4480	0	303	500	100	[47]
DOPS/Na^+	Slipids [38]	288	11232	0	303	200	100	[48]

[a]Number of lipid molecules with largest mole fraction
[b]Number of water molecules
[c]Number of additional cations
[d]Simulation temperature
[e]Total simulation time
[f]Time used for analysis
[g]Reference for simulation files

and glycerol backbone are not well captured by most simulation models [63] and that the cation binding to PC lipid bilayers is overestimated [64]. Based on this data, the cation binding affinity to POPC bilayer was then improved by implicitly including the electronic polarizability using the electronic continuum correction [66].

Here, we collect the set of experimentally measured lipid headgroup and glycerol backbone C-H bond order parameters, which can be used to evaluate the quality of headgroup structure and the ion binding affinity in MD simulations of lipid bilayers containing PS lipids. The available MD simulation models of PS are then compared with the collected experimental data using the NMRlipids open collaboration project (`www.nmrlipids.blogspot.fi`). The results pave the way for the development of lipid force fields with realistic description of the headgroup region of negatively charged lipids in physiological salt conditions. Such models are expected to be useful in understanding biological function of lipid headgroups and glycerol backbone because they behave similarly in model membranes and in bacterial cells [20, 67, 68].

METHODS

C–H bond order parameters from the natural abundance ^{13}C NMR

Headgroup and glycerol backbone C–H bond order parameters of POPS were determined from the chemical-shift resolved dipolar splittings measured with a R-type Proton Detected Local Field (R-PDLF) experiment [90]. The corresponding order parameter signs were measured with a S-DROSS experiment [91] using natural abundance ^{13}C solid state NMR spectroscopy as described previously [92, 93]. The experiments were done in a Bruker Avance III 400 spectrometer operating at a ^{1}H Larmor frequency of 400.03 MHz. Magic angle spinning (MAS) of the sample was used at a frequency of 5.15 kHz (R-PDLF experiment) and 5 kHz (S-DROSS experiment). The following experimental setups were used.

C–H bond order parameters from the R-PDLF experiment. The parameters are described according to Figures 1c and 2c of the original reference for the R-PDLF experiment [90]. The refocused-INEPT delays were $\tau_1 = 1.94$ ms and $\tau_2 = 0.97$ ms. Radio frequency pulses with the nutation frequencies: 46.35

TABLE II: The list of POPC:POPS mixtures simulated with different molar fractions and different amounts of added calcium. The salt concentrations are calculated as [salt]=$N_c \times$[water] / N_w, where [water] = 55.5 M. This corresponds the concentration in buffer before solvating lipids, which are reported in the experiments by Roux et al. [17]. The simulation details are given in the supplementary information.

lipid/counter-ions	force field for lipids / ions	[$CaCl_2$] (M)	[a]N_l	[b]N_w	[c]N_c	[d]T (K)	[e]t_{sim}(ns)	[f]t_{anal} (ns)	[g]files
POPC:POPS (5:1)/K^+	CHARMM36 [22, 61]	0	250:50	11207	0	298	200	180	[69]
POPC:POPS (5:1)/K^+	CHARMM36 [22, 61]	0	110:22	4620	0	298	500	100	[70]
POPC:POPS (5:1)/Na^+	CHARMM36 [22, 61]	0	110:22	4620	0	298	500	100	[71]
POPC:POPS (5:1)	CHARMM36 [22, 60, 61]	0.26	250:50	11190	53	298	200	180	[72]
POPC:POPS (5:1)	CHARMM36 [22, 60, 61]	1.06	250:50	11174	214	298	200	180	[73]
POPC:POPS (1:1)/K^+	CHARMM36 [22, 61]	0	150:150	10785	0	298	200	180	[74]
POPC:POPS (1:0)	MacRog [26]	0	120:0	5120	0	298	200	150	[75]
POPC:POPS (5:1)/K^+	MacRog [26]	0	120:24	5760	0	298	400	250	[76]
POPC:POPS (5:1)/K^+	MacRog [26]	0.10	120:24	5760	10	298	600	300	[76]
POPC:POPS (5:1)/K^+	MacRog [26]	0.30	120:24	5760	31	298	600	300	[76]
POPC:POPS (5:1)/K^+	MacRog [26]	1.00	120:24	5760	104	298	600	300	[76]
POPC:POPS (5:1)/K^+	MacRog [26]	3.00	120:24	5760	311	298	600	300	[76]
POPC:POPS (5:1)/K^+	Lipid14/17 [29, 77]	0	120:24	5760	0	298	500	200	[78]
POPC:POPS (5:1)/Na^+	Lipid14/17 [29, 77]	0	120:24	5760	0	298	500	200	[79]
POPC:POPS (5:1)	Lipid14/17 [29, 77]	0.50	120:24	5760	52	298	300	200	[80]
POPC:POPS (5:1)	Lipid14/17 [29, 77]	1.00	120:24	5760	104	298	300	200	[80]
POPC:POPS (5:1)	Lipid14/17 [29, 77]	2.00	120:24	5760	208	298	300	200	[80]
POPC:POPS (5:1)	Lipid14/17 [29, 77]	3.00	120:24	5760	311	298	300	200	[80]
POPC:POPS (5:1)	Lipid14/17 [29, 77]	4.00	120:24	5760	415	298	300	200	[80]
POPC:POPS (5:1)/Na^+	Lipid14/17 [29, 77]	0	60:12	3600	0	298	1000	1000	[81]
POPC:POPS (5:1)/Na^+	Lipid14/17 [29, 77, 82, 83]	0.08	60:12	3561	5	298	1000	1000	[81]
POPC:POPS (5:1)/Na^+	Lipid14/17 [29, 77, 82, 83]	0.13	60:12	3561	8	298	1000	1000	[81]
POPC:POPS (5:1)/Na^+	Lipid14/17 [29, 77, 82, 83]	0.20	60:12	3561	13	298	1000	1000	[81]
POPC:POPS (5:1)/Na^+	Lipid14/17 [29, 77, 82, 83]	0.41	60:12	3522	26	298	1000	1000	[81]
POPC:POPS (5:1)/Na^+	Lipid14/17 [29, 77, 82, 83]	0.62	60:12	3483	39	298	1000	1000	[81]
POPC:POPS (4:1)/Na^+	Berger [34, 84]	0	102:26	4290	0	310	120	80	[85]
POPC:POPS (4:1)	Berger [34, 84]	0.102[h]	104:24	4306	24	310	300	100	[86]
POPC:POPS (4:1)	Berger [34, 84]	0.715[i]	104:24	4306	72	310	300	100	[87]
POPC:POPS (5:1)/Na^+	GROMOS-CKP [**?**]	0	110:22	?	0	298	500	100	[88]
POPC:POPS (5:1)/Na^+	GROMOS-CKPM [**?**]	0	110:22	?	0	298	500	100	[89]

[a]Number of lipid molecules with largest mole fraction
[b]Number of water molecules
[c]Number of additional cations
[d]Simulation temperature
[e]Total simulation time
[f]Time used for analysis
[g]Reference for simulation files
[h]Calculation of concetration complicated due the scaled ions. Concentration taken as reported in the delivered data.
[i]Calculation of concetration complicated due the scaled ions. Concentration taken as reported in the delivered data.

kHz ($R18_1^7$ pulses), 63.45 kHz (^{13}C 90° and 180°), 50 kHz (SPINAL64 ^1H decoupling pulses). **8.Verb missing. Would it be correct to say: 'Radio frequency pulses had the nutation frequencies:'?** The t_1 increment was equal to 10.79 μs $\times 18 \times 2$, and 32 points in the indirect dimension were recorded using 1024 scans for each, with a recycle delay of 5 s and a spectral with **9.'with' → 'width'?** of 149.5 ppm.

Order parameter signs from the S-DROSS experiment. The parameters are described according to Figures 1b and 1c of the original reference for the S-DROSS experiment [91]. The refocused-INEPT delay δ_2 was 1.19 ms. The τ_1 and τ_2 in the S-DROSS recoupling blocks R were set as $\tau_1 = 39.4\,\mu$s

and τ_2 = 89.4 μs. Radio frequency pulses with the nutation frequencies: 63.45 kHz (^{13}C 90° and 180°), 50 kHz (^{1}H SPINAL64 decoupling). 10.Verb missing. Would it be correct to say: 'Radio frequency pulses had the nutation frequencies:'? The t_1 increment (dipolar recoupling dimension) was 800 μs, and a total of 8 points along t_1 were measured using 1024 scans for each, with a recycle delay of 5 s and a spectral with 11.'with' → 'width'? of 149.5 ppm.

Numerical simulations of S-DROSS curves. The numerical simulations of S-DROSS curves were performed with the SIMPSON simulation package [94] using as input the ^{13}C–^{1}H dipolar couplings, either as determined by the R-PDLF experiments, or as calculated from the known ^{2}H quadrupolar couplings [7]. The chemical shift anisotropy and homonuclear couplings were neglected, and the input file *rep2000* was used to simulate a random distribution of bilayer orientations in the samples studied.

Sample preparation. The sample was prepared simply by mixing the POPS 12.From some company? with water (lipid:water 60:40 wt-%) in an Eppendorf tube by mixing and centrifuging the sample repeatedly until a 13.visually(?) homogeneous viscous fluid was obtained. Then 20 mg of the sample was transferred to an NMR insert suitable for 4 mm NMR rotors. 14.Maybe we need little bit more information about the mixing procedure?

Molecular dynamics simulations

Molecular dynamics simulation data were collected using the Open Collaboration method [63], with the NMRlipids Project blog (`nmrlipids.blogspot.fi`) and GitHub repository (`github.com/NMRlipids/NMRlipidsIVotherHGs`) as the communication platforms. The simulated systems are listed in Tables I (pure PS bilayers without additional ions) and II (mixed PC:PS bilayers at various salt concentrations). Further simulation details are given in the SI. The simulation data are also indexed in a searchable database available at `www.nmrlipids.fi`, and in the NMRlipids/MATCH repository (`github.com/NMRlipids/MATCH`).

The C–H bond order parameters were calculated directly from the carbon and hydrogen positions using the definition

$$S_{\mathrm{CH}} = \frac{1}{2}\langle 3\cos^2\theta - 1\rangle, \qquad (1)$$

where θ is the angle between the C–H bond and the membrane normal (taken to align with z, with bilayer periodic in the xy-plane). Angular brackets denote average over all sampled configurations. The order parameters were first calculated averaging over time separately for each lipid in the system. The average and the standard error of the mean were then calculated over different lipids. Python program (`scripts/calcOrderParameters.py`) that uses the MDAnalysis library [95, 96] is available in Ref. 97. The number density profiles were calculated using the `gmx density` tool of the Gromacs sofware package [98].

Comparison of ion binding to negatively charged lipid bilayers between simulations and experiments using the molecular electrometer

As the order parameters of the α and β carbons in the PC headgroup decrease proportionally to the amount of positive charge bound to the bilayer [99–101], they can be used to measure the ion binding affinity. This concept, known as the molecular electrometer, is especially useful for comparison between simulations and experiments, as the headgroup order parameters at varying cation concentrations can be directly calculated from simulations and compared to the corresponding experimental data [64]. The headgroup order parameters of negatively charged PS and PG lipids also exhibit systematic, but less understood dependencies on the bound charge [17, 102–104]. Therefore, the ion binding affinity to negatively charged bilayers can be better characterized by measuring the PC headgroup order parameters from mixed bilayers [17, 18, 104], see section S2 in the supplementary information.

Before using the PC headgroup order parameters to quantify the ion binding affinity, it is important to quantify their response to a known amount of bound charge [64, 66]. This can be done using experimental data from mixtures of monovalent cationic surfactants (dihexadecyldimethylammonium) and POPC [66, 105], see section S3 in the supplementary information. In this work, we also quantify the response of PC headgroup order parameters to the negatively charged PS headgroups, which also follows the molecular electrometer concept in experiments [68], see section S2 in the supplementary information.

In the experimental ^{2}H NMR literature data used in this work [7, 17], the lipids were first solvated to the buffer and then centrifuged to a pellet that was used in the measurements. Such samples have a lower lipid concentration (approximately 10 wt % of lipids [7, 17, 106]) than gravimetric samples (60 wt %) and simulations (approximately 50-60 wt %) in this work. Larger multilamellar repeat distances are expected in the samples with lower lipid concentrations due to the swelling caused by electrostatic repulsion in pure PS lipid systems [107]. However, the PS headgroup order parameters measured from gravimetric samples in this work are in good agreement with the results from centrifuged samples in the literature [7] (Fig. 2). Furthermore, the equilibrium repeat distance rapidly decreases with the addition of monovalent salts, and is close to the typical simulation box sizes already above 500 mM concentrations [107, 108]. Therefore, the hydration levels of multilamellae are expected to be sufficiently similar in the used simulations and reference experiments.

Two different definitions for the salt concentrations have been used when the molecular electrometer concept is applied to study ion binding affinities. The concentrations are reported either in water before solvating the lipids [17, 64, 99], or in bulk water after solvating the lipids [66, 100]. In this work, we use the former definition to be consistent with the ref-

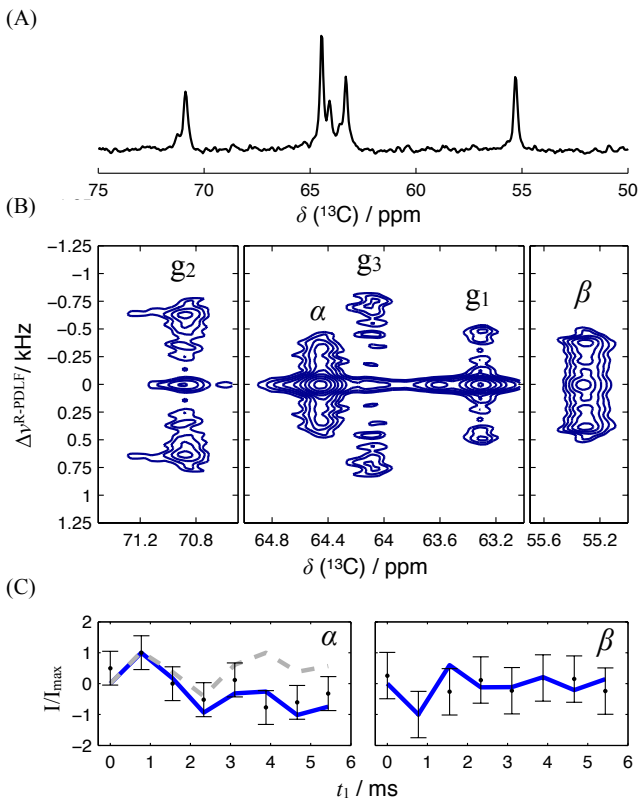

FIG. 1: The headgroup and glycerol backbone region of the (A) INEPT spectrum and (B) 2D R-PDLF spectra. (C) Experimental S-DROSS data (points), and SIMPSON simulations (blue lines) with the order parameter values of -0.12 for the β-carbon, and 0.09 and -0.02 for the α-carbon splittings. Dashed gray line is the S-DROSS curve from a SIMPSON simulation with a positive value (+0.02) for the smaller α-carbon order parameter.

15.I think that the peak labeling would be good to show also in (A).

16.Also for α these are OPs, right, thus we could just exclude the word 'splittings'?

17.Please confirm: Was the positive value used for α in the gray curve 0.02?

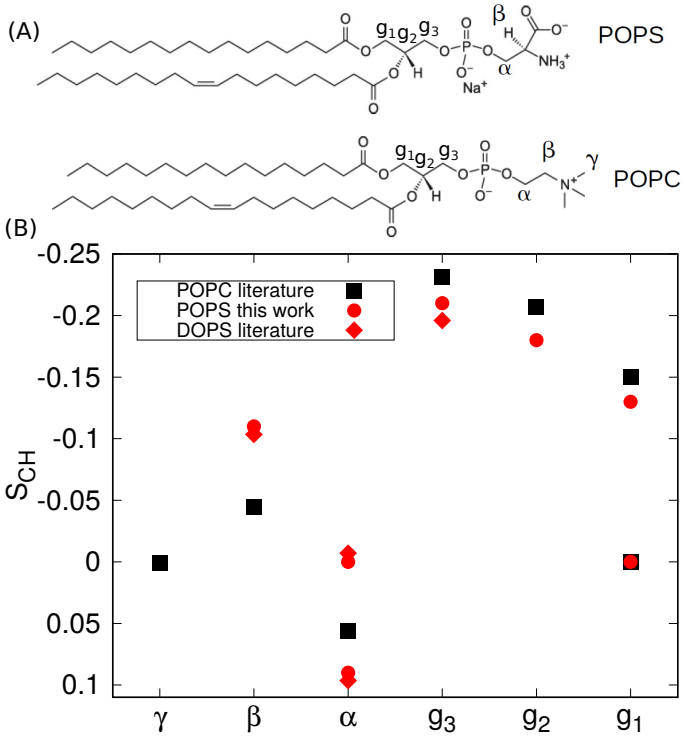

FIG. 2: (A) Chemical structures and labels for the headgroup and glycerol backbone carbons. (B) Headgroup and glycerol backbone order parameters of POPS (T = 298 K) measured in this work compared with the previously published values from DOPS (T = 303 K, ^{2}H NMR, 0.1M of NaCl) [7] and POPC (T = 300 K, ^{13}C NMR) [92] experiments. Signs of the PS order parameters are measured in this work. Signs of the PC order parameters are measured previously [93].

18. 1) Use diamonds for DOPS, spheres for POPS. 2) Error bars? 3) Change the y-label to S_{CH}, and invert the y-axis, as in Fig. 3. 4) Make lower g1 POPC visible, e.g., by slightly larger point.

erence experimental data [17]. The choice of definition has only a marginal effect to the results in simulations with realistic ion binding affinity (section S4 in the supplementary information).

RESULTS AND DISCUSSION

Headgroup and glycerol backbone order parameters of POPS from ^{13}C NMR

The INEPT and 2D R-PDLF experiments from POPS sample give well resolved spectra for all the carbons in the headgroup and glycerol backbone regions (Fig. 1). The glycerol backbone carbon peaks were assigned according to the POPC spectra [92]. The peaks for β and α carbons were assigned according to the known order parameters from the ^{2}H NMR experiments [7]. Slices of the R-PDLF spectra and the resulting order parameter values are shown in the supplementary information (Fig. S6). Since the R-PDLF and previous ^{2}H NMR experiments [7, 18] give only the absolute values of order parameters, we determined the signs of the PS headgroup order parameters using the S-DROSS experiment [91]. The S-DROSS slice clearly shows that the order parameter of the β-carbon is negative (Fig. 1 C)), **19. Could we explain in a few words how this is clearly seen?** which is confirmed by SIMPSON simulations. The beginning of the S-DROSS slice suggests that the larger order parameter of the α-carbon is positive and the deviation towards negative values with longer T_1 times suggests that the smaller order parameter is negative. This is confirmed by a SIMPSON simulation using the value of -0.02 from ^{2}H NMR experiment [18] for the smaller order parameter. The literature value was used because the resolution of our experiment was not sufficient to determine the small value of the order parameter. The S-DROSS curve from SIMPSON simulation with a positive value for the smaller order parameter (dashed grey in Fig. 1 C)) did not agree with the experiment, confirming **20.Or rather 'corroborating'?** the interpretation that the smaller order parameter is negative.

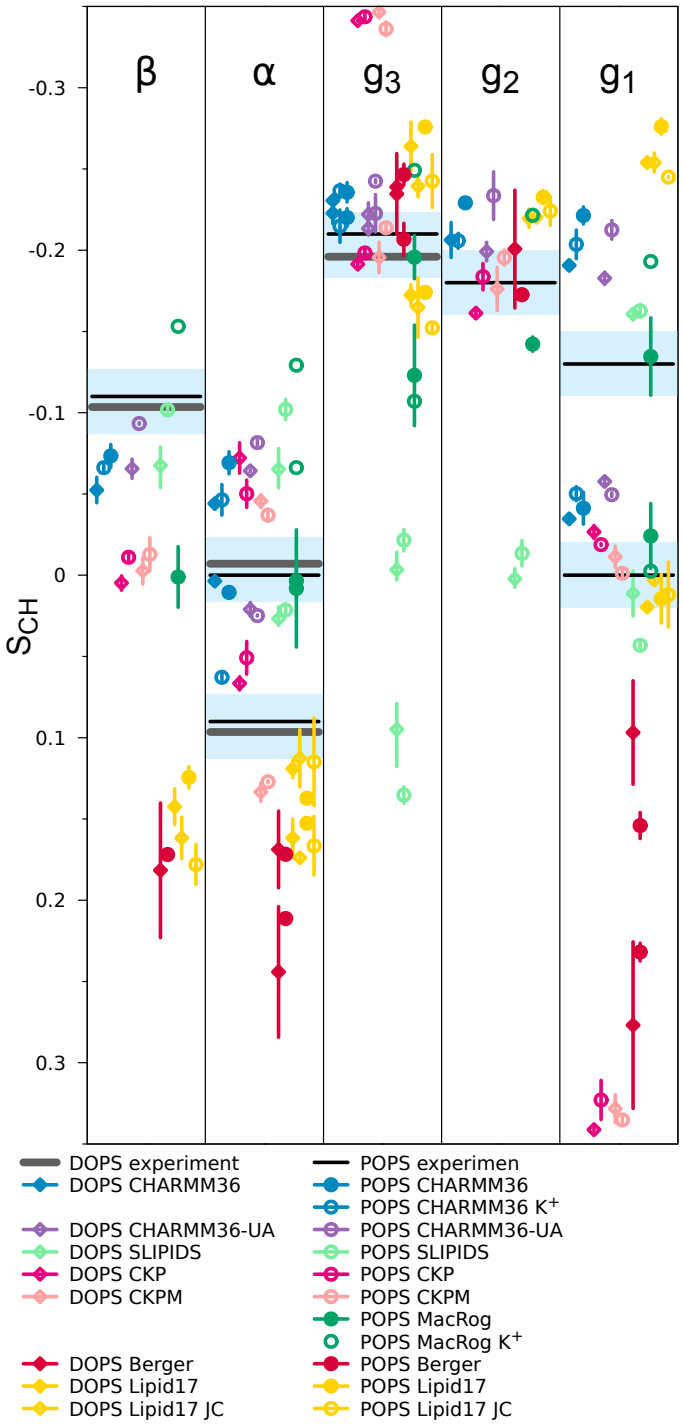

FIG. 3: Order parameters of PS headgroup (β and α) and glycerol backbone (g_3, g_2, g_1) from NMR experiments (horizontal lines), and MD simulations with different force fields (dots). Experimental data for DOPS are measured with 0.1 M of NaCl [7], while all the other data are without additional salt. All the data for DOPS at 303 K and all the data for POPS at 298 K. Light blue areas span 0.04 units around the average of the extremal experimental values, in accordance with the expected quantitative accuracy of experimental values [65]. The vertical bars shown for all simulation values except MacRog K^+ are not error bars, but demonstrate that for these systems we had at least two data sets; the ends of the bars mark the extreme values from the sets, and the dot marks their measurement-time-weighted average.

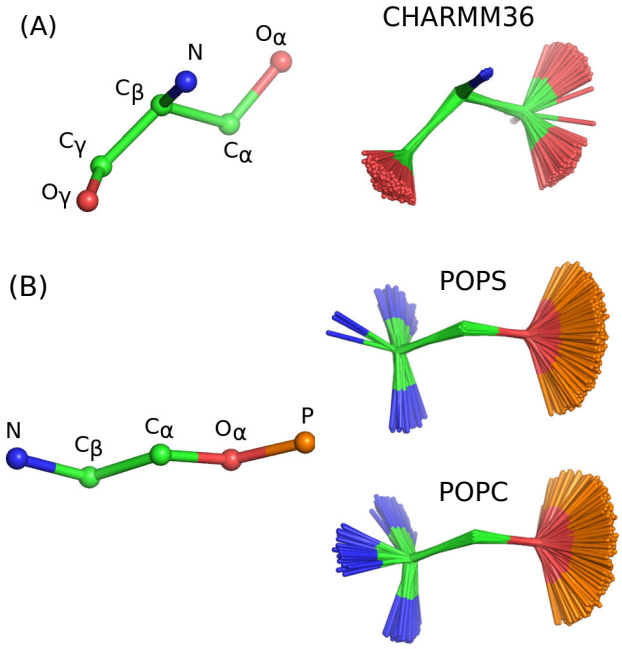

FIG. 4: Overlayed snapshots from CHARMM36 simulations in best agreement with experiments to demonstrate the conformational fluctuations around (A) C_α-C_β-C_γ-O_γ and O_α-C_α-C_β-N of PS headgroup and (B) N-C_β-C_α-O_α and C_β-C_α-O_α-P dihedrals of PS and PC headgroups. The CHARMM36 POPC simulation is from Ref. 109 and Slipids POPC from Ref. 110.

The headgroup and glycerol backbone order parameters of POPS measured in this work are in good agreement with the previously reported values from ^{2}H NMR experiments of DOPS [7] (Fig. 2). When compared with the previously measured values for POPC [92] (Fig. 2), the β-carbon order parameter is significantly more negative and α-carbon experiences a significant forking (different order parameters for the two hydrogens in the same carbon [65]) in the PS headgroup. These features have been intepreted to arise from a rigid PS headgroup conformation, stabilized by hydrogen bonds or electrostatic interactions [7, 8], but detailed structrural interpretation is not available.

Headgroup and glycerol backbone in simulations of PS lipid bilayers without additional ions

The headgroup and glycerol backbone of PS lipids show a wide variety in the order parameters (Fig. 3) and structures (Fig. S9) between different simulation models, as previously observed also for PC lipids [63]. The models perform generally less well for PS than for PC (Figs. 3 and 5 vs. Figs. 2 and 4 in Ref. [63]). Therefore, the interpretation of structural differences between PC and PS headgroups from simulations is not straightforward.

However, if one excludes the glycerol backbone and focuses only on the headgroup (α and β) order parame-

	β	α	g_3	g_2	g_1	Σ
CHARMM 36 K+	M	M	M F	M	**M** F	7
CHARMM 36	M	**M** F	M	M	**M** F	8
CHARMM 36-UA	M	**M**	M	**M**	**M** F	9
MacRog K+	M	**M** F	**M F**	M	M **F**	11
MacRog	**M**	**M F**	**M F**	M	M	14
GROMOS-CKP	**M**	M F	**M F**		**M F**	14
GROMOS-CKPM	**M**	M **F**	**M F**		**M F**	14
Berger	**M**	**M F**	M F		**M** F	14
Slipid	M	**M**	**M F**	**M**	M **F**	14
Lipid17	**M**	**M F**	**M F**	M	**M F**	18
Lipid17 JC	**M**	**M** F	M **F**	M	**M F**	18

FIG. 5: Rough subjective ranking of force fields based on Figure 3. Here ÒMÓ indicates a magnitude problem, ÒFÓ a forking problem; letter size increases with problem severity. Color scheme: Òwithin experimental errorÓ (dark green), Òalmost within experimental errorÓ (light green), Òclear deviation from experimentsÓ (light red), and Òmajor deviation from experimentsÓ (dark red). The Σ-column shows the total deviation of the force field, when individual carbons are given weights of 0 (matches experiment), 1, 2, and 4 (major deviation). For full details of the assessment, see Supplementary Information.

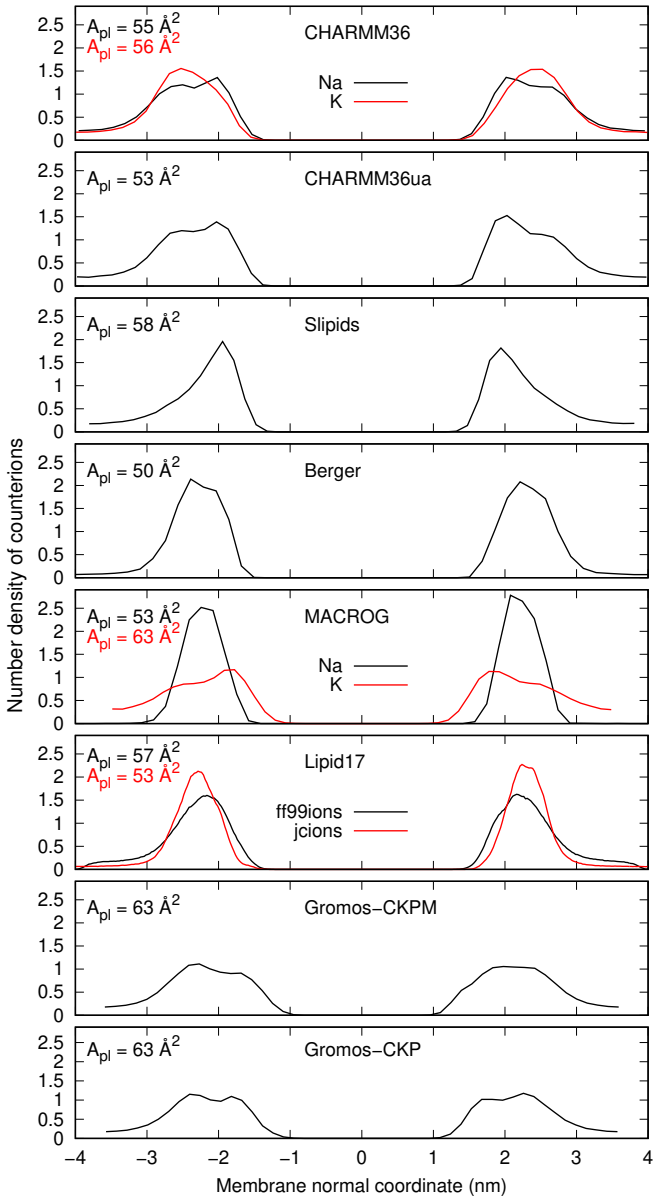

FIG. 6: Counterion densities of POPS lipid bilayer along the membrane normal from simulations with different force fields.

21.Commented by M. Javanainen in blog: MacRog pure POPS is simulated with Verlet cutoff scheme, Piggot is rerunning with group cutoff scheme. Check if affects results & update figures when ready

ters, the best performing models, Slipids, CHARMM36 and CHARMM36ua, do reproduce the larger-than-in-PC forking of the α-carbon. Slipids reproduces also the feature that the β-carbon order parameter in PS is significantly smaller than in PC (Fig. 3 vs. Fig. 2 in Ref. 63). Interestingly, the C_α-C_β-C_γ-O_γ dihedral with a single and narrow peak in the angle distribution close to 120° is more restricted in the best three models than in other models which give two maxima with different angles (Fig. S7). The restricted motion is also visible in the sampled conformations (Figs. 4 (A) and S9) suggesting that the rotation of the carboxyl group is limited in the serine headgroup. In addition, the N-C_β-C_α-O_α dihedral exhibits a more asymmetric and restricted angle distribution for PS than for PC headgroup in CHARMM36 simulations in best agreement with experiments (Figs. 4 (B) and S10). The results might manifest the increased rigidity anticipated in the early experimental studies [7, 8]. Also, the sampled conformations of glycerol backbone significantly vary between different simulation models (Figs. S8, S9, S11 and S12), but further analysis is beyond the scope of this work which focuses on the PS

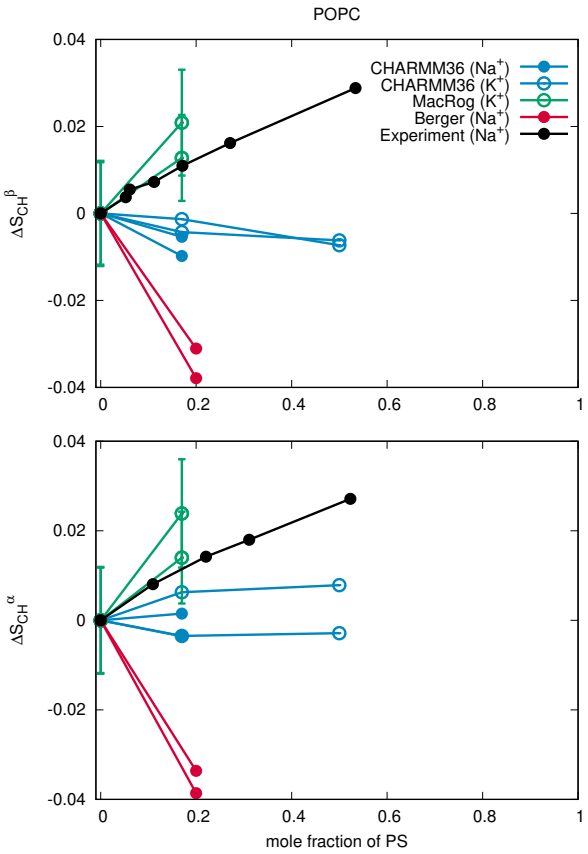

FIG. 7: Changes of POPC headgroup order parameters with increasing amount of POPS in POPC:POPS mixtures at 298 K. Experimental values are from Ref. 68 with the signs measured in Ref. 93.

22.After we know which force field is used for POPC in Gromos-CKP simulations, we might be able to add Gromos-CKP data into this plot.

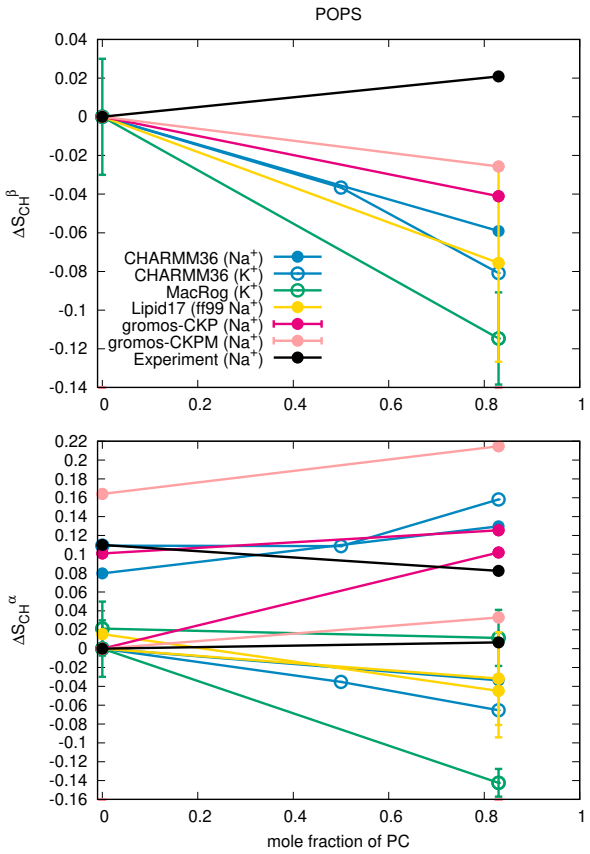

FIG. 8: Changes of POPS headgroup order parameters with increasing amount of POPC in POPC:POPS mixtures at 298 K. Experimental values with the signs are measured for pure POPS system in this work. The signs are assumed to be the same for the mixture and the values are from Ref. 17. The y-axis for the α-carbon results of POPS (bottom) is transferred with the same value for both order parameters such that the lower order parameter value from pure POPS is at zero to correctly illustrate the significant forking.

headgroup.

The suggested characteristic conformations of the PS headgroup may be useful when interpreting experiments and can guide further force field development. However, more accurate MD force fields are required to confirm the suggested conformations because the simulated PS headgroup order parameters are not within the experimental error in any of the tested models.

Counterion binding and interactions between PC and PS headgroups

Membranes containing PS lipids are always accompanied with counterions that modulate electrostatic interactions between lipids and other biomolecules. Counterions are also suggested to screen the repulsion between charged lipid headgroups in MD simulations and thus to reduce the area per lipid of PS bilayers to be smaller than in PC bilayers [34, 50, 51]. Counterion density profiles along membrane normal indicate significant differences between force fields in both binding affinity and distribution of ions in the interface (Fig. 6). The experimental area per lipid (62.7 Å^2) [55] is reproduced only in Gromos-CKP and in the MacRog simulation with potassium counterions, while other models give significantly lower areas (Fig. 6). The counterion binding and the concomitant electrostatic screening of the headgroup repulsion does not fully explain the low area per molecule values, because the MacRog simulation, which has the strongest sodium binding (the lowest concentrations in bulk water), gives the same area per molecule as the CHARMM36ua simulation, which has significantly weaker counterion binding affinity. On the other hand, changing counterions from sodium to potassium, having weaker binding affinity, increases the area per molecule from 53 Å^2 to 63 Å^2 in MacRog simulations. In conclusion, the results are in line with the previous study suggesting that the low areas per molecule in PS lipid bilayers originate from the combination of both counterion binding and hydrogen bonding network between lipid headgroups [111].

Binding of cations to zwitterionic PC lipid bilayers has been

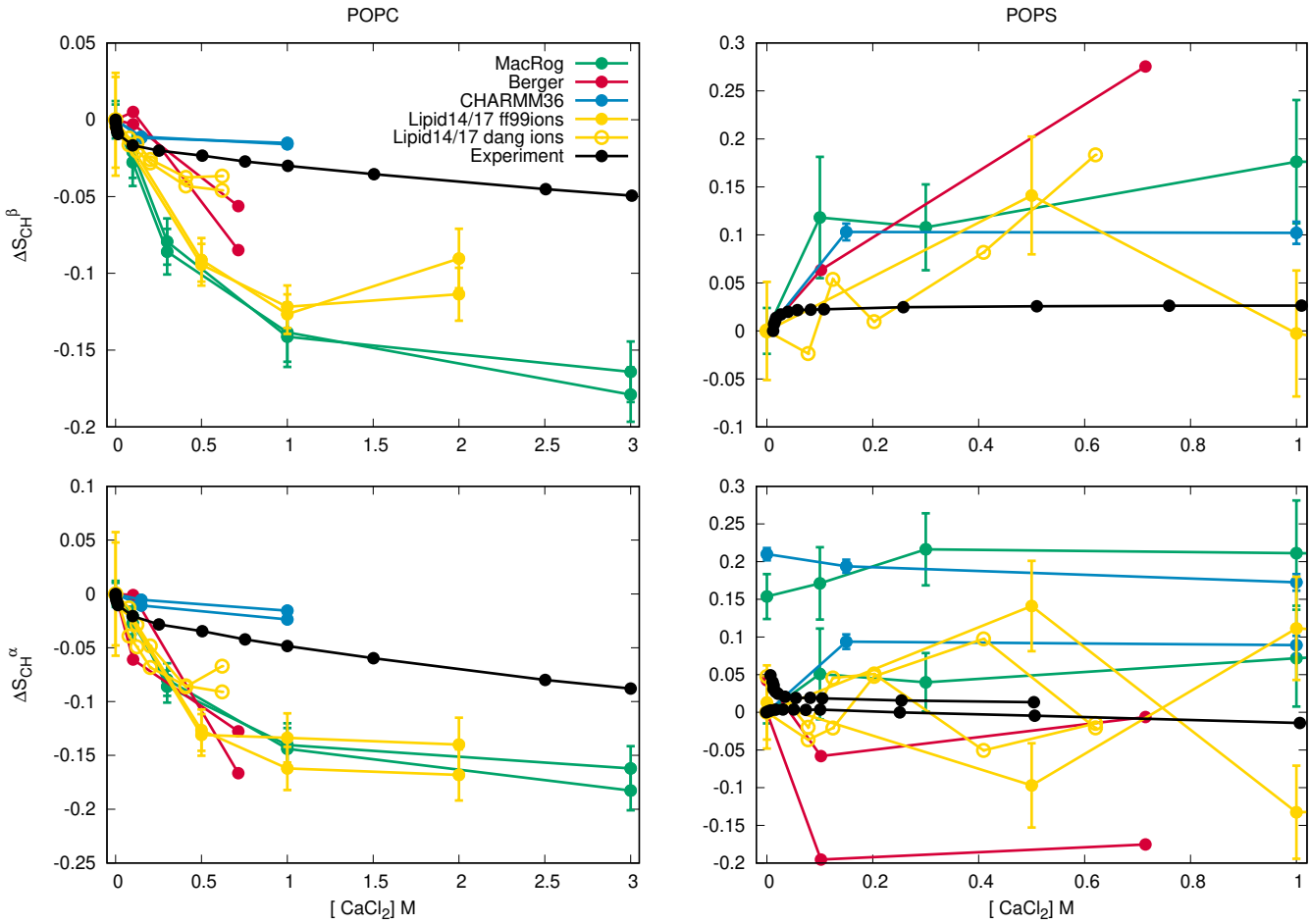

FIG. 9: Changes of POPC (left) and POPS (right) headgroup order parameters from POPC:POPS (5:1) mixture as a function $CaCl_2$ concentration from experiments [17] and different simulations at 298K (except the data for Berger model is from simulation of POPC:POPS (4:1) mixture at 310K [57, 112]). The order parameter values from systems without calcium are set as the zero point of y-axis, except for the α-carbon order parameter of POPS (bottom, right) for which the both order parameters are shifted such that the lower order parameter is zero without additional ions to correctly illustrate the forking with different concentrations of calcium. Potassium counterions are used in MacRog simulations and sodium counterions in Lipid14/17 simulations. In CHARMM36 and Berger simulation with added calcium, the charge is neutralized with calcium and monovalent counterions are not present.

previously evaluated against experiments using the changes of headgroup order parameters as a function of salt concentration [64]. Studying binding of cations to negatively charged lipid bilayers is less straighforward, because the cationic counterions are always present and the ion-free reference state does thus not exist. In addition, the analysis is complicated by the artificial aggregation of counterions in solution observed in some simulations (section S7 in the supplementary information). Therefore, we evaluate here the amount of bound charge not by adding salt (although also this is discussed in the section S7 in the supplementary information), but by studying the changes of the headgroup order parameters with increasing amount of negatively charged lipids (and thus increasing amount of cationic counterions) in the bilayer. According to the molecular electrometer concept, the headgroup order parameters of POPC increase when negatively charged POPS lipids are incorporated in lipid bilayer (section S1) [68, 101]. This is reproduced in the MacRog simulations with potassium counterions (Fig. 7), which have the weakest binding affinity to POPS lipid bilayers (Fig. 6). The CHARMM36 and Berger simulations predict no change, or a decrease, in the POPC headgroup order parameters as a function of increased amount of POPS (Fig. 7). This can be explained by the stronger counterion binding affinity, which cancels the effect of negatively charged headgroups and prevents the experimentally observed increase of headgroup order parameters with increasing amount of PS lipids. Therefore, we suggest that the relatively weak binding of potassium in the MacRog simulations (Fig. 6) predicts the most realistic surface charge density in membranes containing PS lipids, while the other tested simulation models overestimate the counterion binding affinity. The results are in line with the changes of headgroup

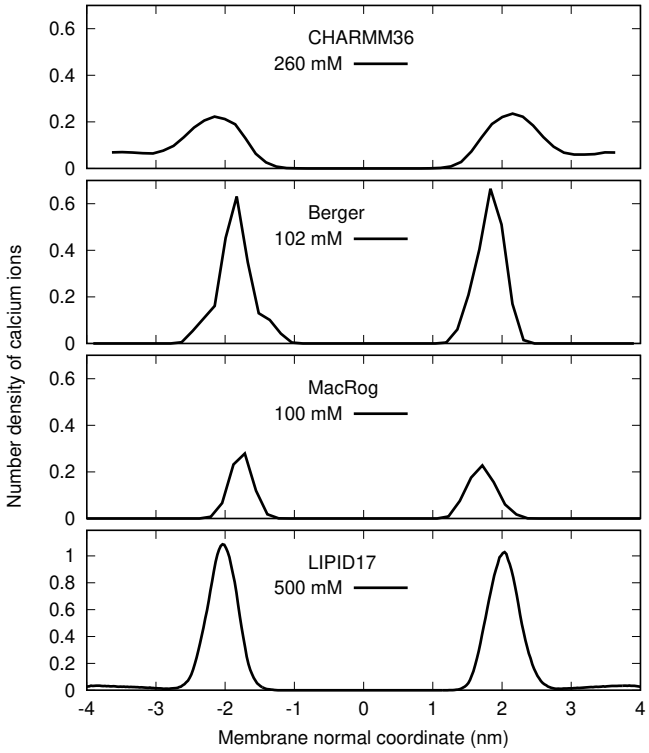

FIG. 10: Number density profiles of Ca^{2+} from POPC:POPS (5:1) mixtures simulated with different force fields. The smallest simulated $CaCl_2$ concentrations are shown. For the density profiles from all the simulated concentrations see figure S18 in the supplementary information.

23.Should we include also counterions into the plot?

order parameters as a function of added counterions analyzed in section S7 in the supplementary information.

The reduced forking of the POPS α-carbon (Fig. 8) together with other experimental results suggest less rigid structure of PS headgroups when diluted with POPC [7, 8, 17, 18, 68]. None of the tested models reproduce the changes of POPS headgroup order parameters with increasing amount of POPC in POPC:POPS mixtures (Fig. 8). Therefore, we conclude that more accurate force fields are necessary to correctly describe the PC-PS headgroup interactions in MD simulations.

Ca^{2+} binding affinity to bilayers with negatively charged PS lipids

Calcium binding affinity to membranes containing the negative charged PS lipids can be experimentally measured by detecting the PC lipid headgroup order parameters from POPC:POPS (5:1) mixtures (section S2), where the dehydrated lipid-ion complexes and phase separation are not observed [15–18]. Despite the lack of an ion-free reference state in the presence of negatively charged lipids, our simulations give coherent results for POPC headgroup order parameters as a function of $CaCl_2$ in the POPC:POPS (5:1) mixtures (Fig. 9). As expected from the previous study of pure PC lipid bilayers [64], almost all the tested simulation models overestimate the experimentally observed [17] decrease of the POPC headgroup order parameters in POPC:POPS (5:1) mixtures as a function of Ca^{2+} concentration (Fig. 9), indicating overestimated calcium binding affinity. The only exception is the CHARMM36 model with the NBfix interaction employed for calcium [60], which underestimates the changes in order parameters, indicating weaker binding affinity than experiments. Notably, CHARMM36 simulations with the NBfix corrections [22, 60] give similar binding affinities of calcium and sodium to POPC bilayer (see section S8), in contrast to the experimental data [99, 100, 113]. Therefore, we conclude that the calcium binding affinity is underestimated in CHARMM36 simulations with the NBfix for calcium [60], but overestimated in all the other tested models. This is evident in the calcium density distributions along membrane normal, where almost all Ca^{2+} ions bind to the membrane interface in all simulation models except CHARMM36 (Fig. 10).

The headgroup order parameters of POPS experimentally measured from a POPC:POPS (5:1) mixture exhibit a strong dependence of $CaCl_2$ with small concentrations and rapid saturation below 100 mM (Fig. 9). In experiments, the order parameter of the POPS β-carbon increases with added $CaCl_2$, whereas the larger α-carbon order parameter decreases; a slight increase is observed in the smaller α-carbon. All these changes are significantly overestimated in the tested simulation models, including CHARMM36 with underestimated binding affinity. In addition, different simulation models predict qualitatively different behaviour for the POPS α-carbon order parameters with added calcium. For example, both order parameters decrease in Berger, but increase in MacRog, and in Lipid14/17 and CHARMM36 a more complicated behavior is seen. This is in contrast to the PC headgroup, where qualitatively correct reponse to bound ions is observed in all simulation models, despite significant discrepancies in the headgroup structure without additional ions [64]. Therefore, we conclude that improvement of force fields is necessary to correctly describe interactions between the PS headgroup and calcium ions in MD simulations.

CONCLUSIONS

Lipids with PS headgroups and their interactions with ions play an important role in lipid mediated signaling processes [2, 4]. Recent studies using molecular dynamics simulations to interpret the various spectroscopic data give contradictory results for the calcium binding details to PS headgroups [57–59]. Here, we used the headgroup C-H bond order parameters and open collaboration method to evaluate the quality of headgroup structure and ion binding affinity to PS lipids in available MD simulation force fields, as previously done for PC lipids [63, 64]. The main advantage of this approach is the direct connection between accurately measured experimental

order parameters and simulations which reduces the ambiguity in the interpretation of experiments.

First, we complemented the available experimental data of PS lipid headgroup order parameters [7, 17] by measuring the signs of the order parameters. None of the available force fields tested using the NMRlipids open collaboration was accurate enough to reproduce the PS headgroup order parameters with the experimental accuracy, but the best models suggested a characteristic rigid conformation for the carboxyl group in the serine headgroup. Comparison to the previously measured headgroup order parameters from POPC:POPS (5:1) bilayers with different ion concentrations [17] showed that the tested MD simulation force fields overestimate the cation binding affinity to the negatively charged bilayers containing PS lipids with two exceptions. The apparently most realisitic monovalent ion binding affinity to PS containing lipid bilayers was observed in the MacRog simulations with potassium counterions and the CHARMM36 force field with recently introduced NBfix correction for calcium [60] underestimated the calcium binding affinity. However, the experimentally measured trends of the PS headgroup order parameter response to the bound calcium and to the dilution of bilayer with zwitterionic PC lipids were not qualitatively reproduced in any of the tested force fields, indicating that improvements in the MD simulation force fields are necessary to study interactions between PS lipids and other biomolecules. This is different to the previous results with PC lipids, where the experimentally measured headgroup order parameter responses to the bound charge were qualitative reproduced even thought the headgroup structures without ions were not correct and the cation binding affinities were overestimated [64].

Our results pave the way for the development of better MD simulations force fields for PS lipids. Using the headgroup order parameters, we were able to evaluate the quality of various conformational ensembles in different force fields. This can guide the development of force fields that would correctly reproduce the conformations sampled by PS headgroups. The experimental dataset of headgroup order parameters from POPC:POPS (5:1) mixture with different cation concentrations can be used to improve cation binding details in the force fields, as recently demonstrated for POPC using the electronic continuum correction [66]. Similar study for POPS is progressed separately [114].

OHSO acknowledges financial support from Academy of Finland (315596), Integrated Structural Biology Research Infrastructure of Helsinki Institute of Life Science (Instruct-HiLIFE), and CSC-IT center for science for computational resources. MJ acknowledges financial support from the Emil Aaltonen foundation and and CSC-IT center for science for computational resources.

* samuli.ollila@helsinki.fi

[1] M. A. Lemmon, Nat. Rev. Mol. Cell Biol. **9**, 99 (2008).
[2] P. A. Leventis and S. Grinstein, Annual Review of Biophysics **39**, 407 (2010).
[3] L. Li, X. Shi, X. Guo, H. Li, and C. Xu, Trends in Biochemical Sciences **39**, 130 (2014), ISSN 0968-0004.
[4] T. Yeung, G. E. Gilbert, J. Shi, J. Silvius, A. Kapus, and S. Grinstein, Science **319**, 210 (2008).
[5] H. Zhao, E. K. J. Tuominen, and P. K. J. Kinnunen, Biochemistry **43**, 10302 (2004).
[6] G. P. Gorbenko and P. K. Kinnunen, Chemistry and Physics of Lipids **141**, 72 (2006).
[7] J. L. Browning and J. Seelig, Biochemistry **19**, 1262 (1980).
[8] G. Büldt and R. Wohlgemuth, The Journal of Membrane Biology **58**, 81 (1981), ISSN 1432-1424, URL http://dx.doi.org/10.1007/BF01870972.
[9] H. Hauser, E. Finer, and A. Darke, Biochemical and Biophysical Research Communications **76**, 267 (1977), ISSN 0006-291X, URL http://www.sciencedirect.com/science/article/pii/0006291X77907215.
[10] R. J. Kurland, Biochemical and Biophysical Research Communications **88**, 927 (1979), ISSN 0006-291X, URL http://www.sciencedirect.com/science/article/pii/0006291X79914979.
[11] M. Eisenberg, T. Gresalfi, T. Riccio, and S. McLaughlin, Biochemistry **18**, 5213 (1979).
[12] H. Hauser and G. G. Shipley, Biochemistry **22**, 2171 (1983).
[13] R. Dluhy, D. G. Cameron, H. H. Mantsch, and R. Mendelsohn, Biochemistry **22**, 6318 (1983).
[14] H. Hauser and G. Shipley, Biochimica et Biophysica Acta (BBA) - Biomembranes **813**, 343 (1985), ISSN 0005-2736, URL http://www.sciencedirect.com/science/article/pii/0005273685902512.
[15] G. W. Feigenson, Biochemistry **25**, 5819 (1986).
[16] J. Mattai, H. Hauser, R. A. Demel, and G. G. Shipley, Biochemistry **28**, 2322 (1989).
[17] M. Roux and M. Bloom, Biochemistry **29**, 7077 (1990).
[18] M. Roux and M. Bloom, Biophys. J. **60**, 38 (1991).
[19] J. M. Boettcher, R. L. Davis-Harrison, M. C. Clay, A. J. Nieuwkoop, Y. Z. Ohkubo, E. Tajkhorshid, J. H. Morrissey, and C. M. Rienstra, Biochemistry **50**, 2264 (2011).
[20] J. Seelig, Cell Biology International Reports **14**, 353 (1990), ISSN 0309-1651, URL http://www.sciencedirect.com/science/article/pii/030916519091204H.
[21] C. G. Sinn, M. Antonietti, and R. Dimova, Colloids and Surfaces A: Physicochemical and Engineering Aspects **282-283**, 410 (2006), a Collection of Papers in Honor of Professor Ivan B. Ivanov (Laboratory of Chemical Physics and Engineering, University of Sofia) Celebrating his Contributions to Colloid and Surface Science on the Occasion of his 70th Birthday.
[22] R. M. Venable, Y. Luo, K. Gawrisch, B. Roux, and R. W. Pastor, The Journal of Physical Chemistry B **117**, 10183 (2013).
[23] T. Piggot, *CHARMM36 POPS simulations (versions 1 and 2) 298 K 1.0 nm LJ switching* (2017), URL https://doi.org/10.5281/zenodo.1129415.
[24] T. Piggot, *CHARMM36 POPS simulations (versions 1 and 2) 298 K 1.0 nm LJ switching with K ions* (2018), URL https://doi.org/10.5281/zenodo.1182654.
[25] T. Piggot, *CHARMM36-UA POPS simulations (versions 1 and 2) 298 K 1.0 nm LJ switching* (2017), URL https://doi.org/10.5281/zenodo.1129458.

[26] A. Maciejewski, M. Pasenkiewicz-Gierula, O. Cramariuc, I. Vattulainen, and T. Róg, J. Phys. Chem. B **118**, 4571 (2014).

[27] T. Piggot, *MacRog POPS simulations (versions 1 and 2) 298 K with corrected PO not OP tails* (2018), URL https://doi.org/10.5281/zenodo.1283335.

[28] M. Javanainen, *Simulation of a POPS membrane with potassium counterions* (2018), URL https://doi.org/10.5281/zenodo.1434990.

[29] I. Gould, A. Skjevik, C. Dickson, B. Madej, and R. Walker, *Lipid17: A comprehensive amber force field for the simulation of zwitterionic and anionic lipids* (2018), in preparation.

[30] I. S. Joung and T. E. Cheatham, The Journal of Physical Chemistry B **112**, 9020 (2008).

[31] M. S. Miettinen and B. Kav, *Molecular dynamics simulation trajectory of an anionic lipid bilayer: 100 mol% POPS with Na+ counterions using Joung-Cheatham Ions* (2018), B.K. acknowledges financial support from International Max Planck Research School on Multiscale Bio-Systems., URL https://doi.org/10.5281/zenodo.1148495.

[32] J. Åqvist, J. Phys. Chem. **94**, 8021 (1990).

[33] M. S. Miettinen and B. Kav, *Molecular dynamics simulation trajectory of an anionic lipid bilayer: 100 mol% POPS with Na+ counterions using ff99 ions* (2018), B.K. acknowledges financial support from International Max Planck Research School on Multiscale Bio-Systems, URL https://doi.org/10.5281/zenodo.1134869.

[34] P. Mukhopadhyay, L. Monticelli, and D. P. Tieleman, Biophysical Journal **86**, 1601 (2004).

[35] T. Piggot, *Berger POPS simulations (versions 1 and 2) 298 K 1.0 nm cut-off* (2017), URL https://doi.org/10.5281/zenodo.1129425.

[36] T. Piggot, *GROMOS-CKP POPS simulations (versions 1 and 2) 298 K with Berger/Chiu NH3 charges and PME* (2017), URL https://doi.org/10.5281/zenodo.1129431.

[37] T. Piggot, *GROMOS-CKP POPS simulations (versions 1 and 2) 298 K with GROMOS NH3 charges and PME* (2017), URL https://doi.org/10.5281/zenodo.1129435.

[38] J. P. M. Jämbeck and A. P. Lyubartsev, Phys. Chem. Chem. Phys. **15**, 4677 (2013).

[39] T. Piggot, *Slipids POPS simulations (versions 1 and 2) 298 K 1.0 nm cut-off with LJ-PME* (2017), URL https://doi.org/10.5281/zenodo.1129441.

[40] T. Piggot, *CHARMM36 DOPS simulations (versions 1 and 2) 303 K 1.0 nm LJ switching* (2017), URL https://doi.org/10.5281/zenodo.1129411.

[41] T. Piggot, *CHARMM36-UA DOPS simulations (versions 1 and 2) 303 K 1.0 nm LJ switching* (2017), URL https://doi.org/10.5281/zenodo.1129456.

[42] B. Kav and M. S. Miettinen, *Molecular dynamics simulation trajectory of an anionic lipid bilayer: 100 mol% DOPS with Na+ counterions using Joung-Cheetham Ions* (2018), B.K acknowledges financial support from International Max Planck Research School on Multiscale Bio-Systems, URL https://doi.org/10.5281/zenodo.1134871.

[43] B. Kav and M. S. Miettinen, *Molecular dynamics simulation trajectory of an anionic lipid bilayer: 100 mol% DOPS with Na+ counterions using ff99 Ions* (2018), B.K acknowledges financial support from International Max Planck Research School on Multiscale Bio-Systems, URL https://doi.org/10.5281/zenodo.1135142.

[44] T. Piggot, *Berger DOPS simulations (versions 1 and 2) 303 K 1.0 nm cut-off* (2017), URL https://doi.org/10.5281/zenodo.1129419.

[45] T. Piggot, *GROMOS-CKP DOPS simulations (versions 1 and 2) 303 K with Berger/Chiu NH3 charges and PME* (2017), URL https://doi.org/10.5281/zenodo.1129429.

[46] T. Piggot, *GROMOS-CKP DOPS simulations (versions 1 and 2) 303 K with GROMOS NH3 charges and PME* (2017), URL https://doi.org/10.5281/zenodo.1129447.

[47] T. Piggot, *Slipids DOPS simulations (versions 1 and 2) 303 K 1.0 nm cut-off with LJ-PME* (2017), URL https://doi.org/10.5281/zenodo.1129439.

[48] F. Favela-Rosales, *MD simulation trajectory of a fully hydrated DOPS bilayer: SLIPIDS, Gromacs 5.0.4. 2017.* (2017), URL https://doi.org/10.5281/zenodo.495510.

[49] J. J. López Cascales, J. García de la Torre, S. J. Marrink, and H. J. C. Berendsen, The Journal of Chemical Physics **104**, 2713 (1996).

[50] S. A. Pandit and M. L. Berkowitz, Biophysical Journal **82**, 1818 (2002).

[51] U. R. Pedersen, C. Leidy, P. Westh, and G. H. Peters, Biochimica et Biophysica Acta (BBA) - Biomembranes **1758**, 573 (2006).

[52] P. T. Vernier, M. J. Ziegler, and R. Dimova, Langmuir **25**, 1020 (2009).

[53] A. Martín-Molina, C. Rodríguez-Beas, and J. Faraudo, Biophysical Journal **102**, 2095 (2012).

[54] P. Jurkiewicz, L. Cwiklik, A. Vojtíšková, P. Jungwirth, and M. Hof, Biochimica et Biophysica Acta (BBA) - Biomembranes **1818**, 609 (2012).

[55] J. Pan, X. Cheng, L. Monticelli, F. A. Heberle, N. Kucerka, D. P. Tieleman, and J. Katsaras, Soft Matter **10**, 3716 (2014).

[56] S. Vangaveti and A. Travesset, The Journal of Chemical Physics **141**, 245102 (2014).

[57] A. Melcrová, S. Pokorna, S. Pullanchery, M. Kohagen, P. Jurkiewicz, M. Hof, P. Jungwirth, P. S. Cremer, and L. Cwiklik, Sci. Reports **6**, 38035 (2016).

[58] M. L. Valentine, A. E. Cardenas, R. Elber, and C. R. Baiz, Biophysical Journal **115**, 1541 (2018), ISSN 0006-3495, URL http://www.sciencedirect.com/science/article/pii/S0006349518310221.

[59] M. J. Hallock, A. I. Greenwood, Y. Wang, J. H. Morrissey, E. Tajkhorshid, C. M. Rienstra, and T. V. Pogorelov, Biochemistry **0**, null (0), https://doi.org/10.1021/acs.biochem.8b01069, URL https://doi.org/10.1021/acs.biochem.8b01069.

[60] S. Kim, D. Patel, S. Park, J. Slusky, J. Klauda, G. Widmalm, and W. Im, Biophysical Journal **111**, 1750 (2016), ISSN 0006-3495, URL http://www.sciencedirect.com/science/article/pii/S0006349516307615.

[61] J. B. Klauda, R. M. Venable, J. A. Freites, J. W. O'Connor, D. J. Tobias, C. Mondragon-Ramirez, I. Vorobyov, A. D. MacKerell Jr, and R. W. Pastor, J. Phys. Chem. B **114**, 7830 (2010).

[62] O. Berger, O. Edholm, and F. Jähnig, Biophys. J. **72**, 2002 (1997).

[63] A. Botan, F. Favela-Rosales, P. F. J. Fuchs, M. Javanainen, M. Kanduč, W. Kulig, A. Lamberg, C. Loison, A. Lyubartsev, M. S. Miettinen, et al., J. Phys. Chem. B **119**, 15075 (2015).

[64] A. Catte, M. Girych, M. Javanainen, C. Loison, J. Melcr, M. S. Miettinen, L. Monticelli, J. Maatta, V. S. Oganesyan, O. H. S. Ollila, et al., Phys. Chem. Chem. Phys. **18**, 32560 (2016).

[65] O. S. Ollila and G. Pabst, Biochimica et Biophysica Acta (BBA) - Biomembranes **1858**, 2512 (2016).

[66] J. Melcr, H. Martinez-Seara, R. Nencini, J. Kolafa, P. Jungwirth, and O. H. S. Ollila, The Journal of Physical Chemistry

B **122**, 4546 (2018).
[67] H. U. Gally, G. Pluschke, P. Overath, and J. Seelig, Biochemistry **20**, 1826 (1981).
[68] P. Scherer and J. Seelig, EMBO J. **6** (1987).
[69] J. J. Madsen, *MD simulations of bilayers containing PC/PS mixtures and CaCl_2: 150POPC_150POPS_neutral* (2019), URL https://doi.org/10.5281/zenodo.2542164.
[70] T. Piggot, *CHARMM36 POPS/POPC simulations (versions 1 and 2) 298 K 1.0 nm LJ switching with K ions* (2018), URL https://doi.org/10.5281/zenodo.1182658.
[71] T. Piggot, *CHARMM36 POPS/POPC simulations (versions 1 and 2) 298 K 1.0 nm LJ switching with Na ions* (2018), URL https://doi.org/10.5281/zenodo.1182665.
[72] J. J. Madsen, *MD simulations of bilayers containing PC/PS mixtures and CaCl_2: 250POPC_50POPS_0.15MCaCl_2* (2019), URL https://doi.org/10.5281/zenodo.2542176.
[73] J. J. Madsen, *MD simulations of bilayers containing PC/PS mixtures and CaCl_2: 250POPC_50POPS_1MCaCl_2* (2019), URL https://doi.org/10.5281/zenodo.2542135.
[74] J. J. Madsen, *MD simulations of bilayers containing PC/PS mixtures and CaCl_2: 250POPC_50POPS_neutral* (2019), URL https://doi.org/10.5281/zenodo.2542151.
[75] M. Javanainen, *Simulation of a POPC bilayer at 298K, lipid model by Maciejewski and Rog* (2018), URL https://doi.org/10.5281/zenodo.1167532.
[76] M. Javanainen, *Simulations of popc/pops membranes with cacl_2.* (2017), URL https://doi.org/10.5281/zenodo.1409551.
[77] C. J. Dickson, B. D. Madej, A. A. Skjevik, R. M. Betz, K. Teigen, I. R. Gould, and R. C. Walker, J. Chem. Theory Comput. **10**, 865 (2014).
[78] B. Kav and M. S. Miettinen, *Amber Lipid17 Simulations of POPC/POPS Membranes with KCl Counterions* (2018), B.K acknowledges financial support from International Max Planck Research School on Multiscale Bio-Systems, URL https://doi.org/10.5281/zenodo.1250969.
[79] B. Kav and M. S. Miettinen, *Amber Lipid17 Simulations of POPC/POPS Membranes with NaCl Counterions* (2018), B.K acknowledges financial support from International Max Planck Research School on Multiscale Bio-Systems, URL https://doi.org/10.5281/zenodo.1250975.
[80] B. Kav and M. S. Miettinen, *Amber Lipid17 Simulations of POPC/POPS Membranes with CaCl2* (2018), B.K acknowledges financial support from International Max Planck Research School on Multiscale Bio-Systems, URL https://doi.org/10.5281/zenodo.1438848.
[81] J. Melcr, *Molecular dynamics simulations of lipid bilayers containing POPC and POPS with the lipid17 force field, only counterions, and CaCl2 concentrations* (2018), URL https://doi.org/10.5281/zenodo.1487761.
[82] D. E. Smith and L. X. Dang, J. Chem. Phys **100**, 3757 (1994), URL http://scitation.aip.org/content/aip/journal/jcp/100/5/10.1063/1.466363.
[83] L. X. Dang, G. K. Schenter, V.-A. Glezakou, and J. L. Fulton, J. Phys. Chem. B **110**, 23644 (2006), ISSN 1520-6106, URL http://dx.doi.org/10.1021/jp064661f.
[84] D. P. Tieleman, H. J. Berendsen, and M. S. Sansom, Biophys. J. **76**, 1757 (1999).
[85] O. O. H. Samuli, *POPC:POPS (4:1) simulation with Berger model at 310K* (2018), URL https://doi.org/10.5281/zenodo.1475285.
[86] C. Lukasz, *MD simulation trajectory of a POPC/POPS (4:1) bilayer with 102mM CaCl2, Berger force field for lipids, scaled charges for Ca2+ and Cl-* (2017), URL https://doi.org/10.5281/zenodo.887398.
[87] C. Lukasz, *MD simulation trajectory of a POPC/POPS (4:1) bilayer with 715mM CaCl2, Berger force field for lipids, scaled charges for Ca2+ and Cl-* (2017), URL https://doi.org/10.5281/zenodo.887400.
[88] T. Piggot, *GROMOS-CKP POPS/POPC simulations (versions 1 and 2) 298 K with GROMOS NH3 charges and PME* (2018), URL https://doi.org/10.5281/zenodo.1283333.
[89] T. Piggot, *GROMOS-CKP POPS/POPC simulations (versions 1 and 2) 298 K with Berger/Chiu NH3 charges and PME* (2018), URL https://doi.org/10.5281/zenodo.1283331.
[90] S. V. Dvinskikh, H. Zimmermann, A. Maliniak, and D. Sandstrom, J. Magn. Reson. **168**, 194 (2004).
[91] J. D. Gross, D. E. Warschawski, and R. G. Griffin, J. Am. Chem. Soc. **119**, 796 (1997).
[92] T. M. Ferreira, F. Coreta-Gomes, O. H. S. Ollila, M. J. Moreno, W. L. C. Vaz, and D. Topgaard, Phys. Chem. Chem. Phys. **15**, 1976 (2013).
[93] T. M. Ferreira, R. Sood, R. Bärenwald, G. Carlström, D. Topgaard, K. Saalwächter, P. K. J. Kinnunen, and O. H. S. Ollila, Langmuir **32**, 6524 (2016).
[94] M. Bak, J. T. Rasmussen, and N. C. Nielsen, Journal of Magnetic Resonance **147**, 296 (2000), ISSN 1090-7807, URL http://www.sciencedirect.com/science/article/pii/S1090780700921797.
[95] N. Michaud-Agrawal, E. J. Denning, T. B. Woolf, and O. Beckstein, Journal of Computational Chemistry **32**, 2319 (2011), https://onlinelibrary.wiley.com/doi/pdf/10.1002/jcc.21787, URL https://onlinelibrary.wiley.com/doi/abs/10.1002/jcc.21787.
[96] Richard J. Gowers, Max Linke, Jonathan Barnoud, Tyler J. E. Reddy, Manuel N. Melo, Sean L. Seyler, Jan Domański, David L. Dotson, Sébastien Buchoux, Ian M. Kenney, et al., in *Proceedings of the 15th Python in Science Conference*, edited by Sebastian Benthall and Scott Rostrup (2016), pp. 98 – 105.
[97] ohsOllila and et al., *Match github repository*, URL https://github.com/NMRLipids/MATCH.
[98] M. Abraham, D. van der Spoel, E. Lindahl, B. Hess, and the GROMACS development team, *GROMACS user manual version 5.0.7* (2015), URL www.gromacs.org.
[99] H. Akutsu and J. Seelig, Biochemistry **20**, 7366 (1981).
[100] C. Altenbach and J. Seelig, Biochemistry **23**, 3913 (1984).
[101] J. Seelig, P. M. MacDonald, and P. G. Scherer, Biochemistry **26**, 7535 (1987).
[102] F. Borle and J. Seelig, Chemistry and Physics of Lipids **36**, 263 (1985).
[103] P. M. Macdonald and J. Seelig, Biochemistry **26**, 1231 (1987).
[104] M. Roux and J.-M. Neumann, FEBS Letters **199**, 33 (1986).
[105] P. G. Scherer and J. Seelig, Biochemistry **28**, 7720 (1989).
[106] M. Roux, J.-M. Neumann, M. Bloom, and P. F. Devaux, European Biophysics Journal **16**, 267 (1988).
[107] M. Loosley-Millman, R. Rand, and V. Parsegian, Biophysical Journal **40**, 221 (1982).
[108] R. Rand and V. Parsegian, Biochimica et Biophysica Acta (BBA) - Reviews on Biomembranes **988**, 351 (1989).
[109] J. Melcr, *POPC lipid membrane, 303K, Charmm36 force field, simulation files and 200 ns trajectory for Gromacs MD simu-*

lation engine v5.1.2 (2016), URL https://doi.org/10.5281/zenodo.153944.

[110] F. Favela-Rosales, *MD simulation trajectory of a lipid bilayer: Pure POPC in water. SLIPIDS, Gromacs 4.6.3. 2016.* (2016), URL https://doi.org/10.5281/zenodo.166034.

[111] H. I. Petrache, S. Tristram-Nagle, K. Gawrisch, D. Harries, V. A. Parsegian, and J. F. Nagle, Biophysical Journal **86**, 1574 (2004).

[112] S. Ollila, M. T. Hyvönen, and I. Vattulainen, J. Phys. Chem. B **111**, 3139 (2007).

[113] G. Cevc, Biochim. Biophys. Acta - Rev. Biomemb. **1031**, 311 (1990).

[114] Melcr and et al., *Eccpops github repository*, URL https://github.com/jmelcr/ecc_lipids.

ToDo

P.

1. Authorlist is not yet complete . . . 1
2. Correct citation for CHARMMua DOPS . . . 2
3. Correct citation(s) for CKP. . . . 2
4. Correct citation(s) for CKP. . . . 2
5. Correct citation for CHARMMua DOPS . . . 2
6. Correct citation(s) for CKP. . . . 2
7. Correct citation(s) for CKP. . . . 2
8. Verb missing. Would it be correct to say: 'Radio frequency pulses had the nutation frequencies:'? . . . 3
9. 'with' → 'width'? . . . 3
10. Verb missing. Would it be correct to say: 'Radio frequency pulses had the nutation frequencies:'? . . . 4
11. 'with' → 'width'? . . . 4
12. From some company? . . . 4
13. visually(?) . . . 4
14. Maybe we need little bit more information about the mixing procedure? . . . 4
15. I think that the peak labeling would be good to show also in (A). . . . 5
16. Also for α these are OPs, right, thus we could just exclude the word 'splittings'? . . . 5
17. Please confirm: Was the positive value used for α in the gray curve 0.02? . . . 5
18. 1) Use diamonds for DOPS, spheres for POPS. 2) Error bars? 3) Change the y-label to S_{CH}, and invert the y-axis, as in Fig. 3. 4) Make lower g1 POPC visible, e.g., by slightly larger point. . . . 5
19. Could we explain in a few words how this is clearly seen? . . . 5
20. Or rather 'corroborating'? . . . 5
21. Commented by M. Javanainen in blog: MacRog pure POPS is simulated with Verlet cutoff scheme, Piggot is rerunning with group cutoff scheme. Check if affects results & update figures when ready . . . 7
22. After we know which force field is used for POPC in Gromos-CKP simulations, we might be able to add Gromos-CKP data into this plot. . . . 8
23. Should we include also counterions into the plot? . 10